Chronic hypoxia up-regulates α_{1H} T-type channels and low-threshold catecholamine secretion in rat chromaffin cells

V. Carabelli[1], A. Marcantoni[1], V. Comunanza[1], A. de Luca, J. Díaz[2], R. Borges[2] and E. Carbone[1]

[1]*Department of Neuroscience, NIS Center of Excellence, CNISM Research Unit,10125 Torino, Italy*
[2]*Department of Physical Medicine and Pharmacology, University de La Laguna, 38071 La Laguna, Spain*

α_{1H} T-type channels recruited by β_1-adrenergic stimulation in rat chromaffin cells (RCCs) are coupled to fast exocytosis with the same Ca^{2+} dependence of high-threshold Ca^{2+} channels. Here we show that RCCs exposed to chronic hypoxia (CH) for 12–18 h in 3% O_2 express comparable densities of functional T-type channels that depolarize the resting cells and contribute to low-voltage exocytosis. Following chronic hypoxia, most RCCs exhibited T-type Ca^{2+} channels already available at −50 mV with the same gating, pharmacological and molecular features as the α_{1H} isoform. Chronic hypoxia had no effects on cell size and high-threshold Ca^{2+} current density and was mimicked by overnight incubation with the iron-chelating agent desferrioxamine (DFX), suggesting the involvement of hypoxia-inducible factors (HIFs). T-type channel recruitment occurred independently of PKA activation and the presence of extracellular Ca^{2+}. Hypoxia-recruited T-type channels were partially open at rest (T-type 'window-current') and contributed to raising the resting potential to more positive values. Their block by 50 μM Ni^{2+} caused a 5–8 mV hyperpolarization. The secretory response associated with T-type channels could be detected following mild cell depolarizations, either by capacitance increases induced by step depolarizations or by amperometric current spikes induced by increased [KCl]. In the latter case, exocytotic bursts could be evoked even with 2–4 mM KCl and spike frequency was drastically reduced by 50 μM Ni^{2+}. Chronic hypoxia did not alter the shape of spikes, suggesting that hypoxia-recruited T-type channels increase the number of secreted vesicles at low voltages, without altering the mechanism of catecholamine release and the quantal content of released molecules.

(Received 14 March 2007; accepted after revision 3 August 2007; first published online 9 August 2007)
Corresponding author E. Carbone: Department of Neuroscience, Corso Raffaello 30, 10125 Torino, Italy.
Email: emilio.carbone@unito.it

T-type Ca^{2+} channels are expressed in a variety of cells, where they control rhythmic cell activity, muscle contraction, hormone release and cell differentiation (Pérez-Reyes, 2003) as well as fast 'low-threshold' exocytosis (Carbone *et al.* 2006). New evidence shows that α_{1H} T-type channels, weakly expressed in adult rat chromaffin cells (RCCs), can be up-regulated following chronic exposure to permeant cAMP and β_1-adrenergic stimulation, through an Epac-mediated PKA-independent pathway (Novara *et al.* 2004). cAMP-recruited α_{1H} channels can sustain secretion at lower depolarizations with the same efficacy of normally expressed high-voltage-gated Ca^{2+} channels (Giancippoli *et al.* 2006).

As recently noticed, T-type channel recruitment and remodelling of cell excitability is part of a gene expression programme in response to stress conditions (Carbone *et al.* 2006). Recruitment of T-type channels has been reported in myocytes during cardiac hypertrophy and heart failure (Nuss & Houser, 1993; Sen & Smith, 1994), smooth muscle cells after vascular injury (Schmitt *et al.* 1995), absence epilepsy and neuronal damage (Chung *et al.* 1993; Tsakiridou *et al.* 1995), prostatic tumour cells, and human myoblasts during differentiation (Bijlenga *et al.* 2000; Mariot *et al.* 2002). T-type channel recruitment also occurs in PC12 cells exposed either to chronic hypoxia (CH) (> 6 h) or to overnight incubation with desferrioxamine (DFX), via hypoxia-inducible factor (HIF-2α) activation (Del Toro *et al.* 2003). To our knowledge, this work is the only one showing a selective up-regulation of α_{1H} channels and no effects on HVA channels during CH. Most reports indicate a preferential increase of L-type current densities in carotid body glomus cells and PC12 cells (Hempleman, 1996; Scragg *et al.* 2005) and a depression

 DOI: 10.1113/jphysiol.2007.132274

in hypertrophied right-ventricular cells (Chouabe *et al.* 1997). We found it curious that CH up-regulates T-type channels only in PC12 cells. A possibility is that low-P_{O_2} may impair T-type channel functioning, but this seems unlikely since acute hypoxia only slightly inhibits the α_{1H} channels stably expressed in HEK-293 cells (Fearon *et al.* 2000) and up-regulates a T-type current in pacemaker neurons of rostral ventrolateral medulla (Sun & Reis, 1994).

Here, in agreement with Del Toro *et al.* (2003), we report that CH effectively recruits low-voltage-activated Ca^{2+} currents that are functionally coupled to low-threshold exocytosis in adult RCCs. The hypoxia-recruited Ca^{2+} currents through a HIF-dependent pathway possess the molecular, pharmacological and gating features of α_{1H} T-type channels. Quantitatively, the T-type channels expressed during CH or DFX incubation induce a depolarization-evoked secretion at low voltages (−50 mV) comparable to that associated with long-term exposures to pCPT-cAMP (Giancippoli *et al.* 2006). In addition, hypoxia-recruited T-type channels enhance the mean frequency of amperometric spikes during small depolarizations in low KCl concentrations (2–10 mM) preserving the kinetic parameters of single exocytic spikes. Our findings uncover a new role for T-type channels in hypoxic RCCs which may explain the increased cardiovascular tone in response to intermittent or sustained CH (Bao *et al.* 1997; Fletcher, 2001) and may be of relevance for neuronal networks (Peña & Ramirez, 2005) and O_2-sensing cells (López-Barneo *et al.* 2003) in which hypoxia-sensitive T-type channels may be critical.

Methods

Cell culture

Chromaffin cells were isolated from the medulla of adrenal glands obtained from adult Sprague-Dawley CD rats (200–300 g), killed by means of cervical dislocation. All experiments were performed in accordance with the guidelines established by the National Council on Animal Care and were approved by the local Animal Care Committee of Turin University. Glands were rapidly removed and bathed in saline (Ca^{2+} and Mg^{2+} free)–Locke solution (mM): 154 NaCl; 3.6 KCl; 5.6 $NaHCO_3$; 5.6 glucose; 10 Hepes, pH 7.3 with NaOH. After removing the cortex, the adrenal medulla was enzymatically treated for 55–70 min at 37°C, adding 110 μl liberase blendzymes III (Roche) to 890 μl Locke solution. The suspension was gently shaken every 10 min, washed twice in a buffer solution of Locke and 1% bovine serum albumin (BSA) and finally centrifuged at 64 g for 4 min. The pellet was resuspended in 1 ml Dulbecco's modified Eagle's medium (DMEM), except where otherwise indicated, enriched with 15% fetal bovine serum, which was previously heat-inactivated. Penicillin (50 IU ml^{-1}), streptomycin (50 μg ml^{-1}) and gentamycin (2.5 μg ml^{-1}) were then added to the culture medium. Isolated RCCs were plated in four-well plastic dishes, treated with poli-DL-ornithine (0.5 mg ml^{-1}) and laminin (5 μg ml^{-1}). Control cells were then incubated in a humidified atmosphere (37°C, 5% CO_2) and used from 1–4 days after plating. Hypoxic conditions were obtained using a CO_2 incubator series CB-150 (Binder GmbH, Tuttlingen, Germany) set at 3% O_2 and balanced with N_2. For experiments in Ca^{2+}-free conditions, RCCs were grown in modified DMEM (deprived of Ca^{2+}) and enriched with 1% insulin–transferrin–selenite solution (ITS; containing insulin 1.0 mg ml^{-1}, transferrin 0.55 mg ml^{-1} and sodium selenite 0.5 μg ml^{-1}).

Voltage-clamp recordings

Ca^{2+} currents and depolarization-evoked capacitance increases were measured as previously described (Carabelli *et al.* 2003; Giancippoli *et al.* 2006) in the perforated-patch configuration using an EPC-9 patch-clamp amplifier (HEKA Elektronik, Lambrecht, Germany). Ca^{2+} currents were sampled at 10 kHz and filtered at 2 kHz; exocytosis was measured as membrane capacitance increases following pulse depolarizations by applying a sinusoidal wave function on the holding potential (±25 mV amplitude, 1 kHz). Fast capacitive transients due to depolarizing pulses were minimized online by the patch-clamp analog compensation. Series resistance was compensated by 80% and monitored during the experiment. Since the drugs applied extracellularly did not affect the liquid junction potential (LJP), the indicated voltages were not corrected for LJP at the interface between the pipette solution and the bath. A major deviation concerns the LJP existing between recordings in solutions used for Ca^{2+} current measurements (135 mM NaCl) and the capacitance increases made in solutions containing 145 mM TEACl in which the LJP is shifted by about 4 mV toward more positive potentials. Experiments were performed at room temperature (22–24°C). Data are given as means ± standard error of the mean (S.E.M.) for n cells. Statistical significance ($P < 0.05$) was calculated by means of Student's t test for unpaired data.

Current clamp experiments

Resting potentials at various KCl concentrations were measured in perforated-patches and current-clamp mode using an Axopatch 200A amplifier (Axon Instruments, Union City, CA, USA). Sampling rate was 10 kHz and traces were filtered at 1 kHz. The external solutions contained different KCl concentrations and were identical to those utilized for the amperometric measurements (see below). At the starting conditions (zero KCl concentration)

the resting potential measured in the absence of membrane current was usually very negative in both normal and hypoxic cells. The cell input resistance was usually high and varied between 1 and 2.6 GΩ.

Amperometric detection of exocytosis

Carbon fibres (5 μm diameter) were purchased from Ala Scientific Instruments Inc. (Westbury, NY, USA). Electrochemical recordings were performed using a HEKA EPC-10 amplifier. Amperometric measurements were performed by gently positioning the carbon fibre microelectrode (polarized at +800 mV) adjacent to the cell membrane. Exocytosis was stimulated by perfusing the cells with a solution containing 10 mM $CaCl_2$ and variable concentrations of KCl (2–15 mM). Experiments were carried out when the baseline current was less than 10 pA. Amperometric currents were sampled at 4 kHz, low-pass filtered at 1 kHz, and monitored during 2 min recordings. Data were analysed by IGOR macros (WaveMetrics, Lake Oswego, OR, USA) as described elsewhere (Segura *et al.* 2000). The analysis of individual exocytotic events was done by measuring the following parameters: maximum oxidation current (I_{max}), spike width at half height ($t_{1/2}$), total charge of the spike (Q), ascending slope of the spike (m) and time to reach the spike (t_P). Statistical analysis was performed by the non-parametric Mann–Whitney rank sum or Kolmogorov–Smirnov tests (Machado *et al.* 2001).

Solutions and chemicals

The perforated-patch configuration was obtained using amphotericin B (Sigma, St Louis, MO, USA). Stock solutions dissolved in DMSO (50 mg ml^{-1}) were kept at −20°C; the final concentration in the pipette filling solution was 50–100 μg ml^{-1} (Cesetti *et al.* 2003). If not specifically indicated, for all the experiments the pipette filling solution was (mM): 135 $CsMeSO_3$, 8 NaCl, 2 $MgCl_2$, 20 Hepes, pH 7.3 with CsOH. Ca^{2+} currents were recorded with an extracellular solution deprived of KCl (in order to minimize steady T-type channel inactivation) and containing (mM) 135 NaCl, 2 $MgCl_2$, 10 Hepes, 10 glucose, 5 $CaCl_2$, pH 7.3 with NaOH. Tetrodotoxin (TTX, 300 nM) was added to the external solution to block Na^+ currents. For capacitance increases recordings, due to the slowing of Na^+ gating currents induced by TTX, the external solution was similar to that used previously, containing (mM): 145 TEACl, 5 $CaCl_2$, 10 Hepes, 10 glucose, pH 7.3 with CsOH (Giancippoli *et al.* 2006). For amperometric and current-clamp recordings cells were initially kept in a KCl-free solution (130 NaCl, 2 $MgCl_2$, 10 Hepes, 10 glucose, 10 $CaCl_2$) and then, secretion was induced by increasing KCl to 2, 4, 10 and 15 mM and reducing NaCl concentration proportionally. When specified, $NiCl_2$ (50 μM) was added to the extracellular solution.

Rp-cAMPS (Rp-adenosine 3_, 5_-cyclic-monophosphorothioate triethylammonium salt), desferrioxamine mesylate salt (DFX), mibefradil dihydrochloride hydrate and nifedipine were purchased from Sigma. The PKA inhibitor H89 was obtained from CN Biosciences Inc. (Darmstadt, Germany). ω-CTx-GVIA and ω-Aga-IVA toxins were purchased from the Peptide Institute (Osaka, Japan).

RNA extraction and reverse transcription-polymerase chain reaction (RT-PCR)

Total RNA was isolated from both control and chromaffin cells exposed to CH (16–18 h, 3%O_2) of adult rats with the RNeasy Micro Kit (Qiagen AG, Basel, Switzerland) as indicated in the manufacturer's instructions. The DNase-treated total RNA used in the reverse transcription (RT) procedure was extracted from the medulla zone of 12 rat adrenal glands for both the control and treated samples taking extreme care to avoid contamination of cortical regions. It is important to notice that besides a dominant fraction of RCCs, the isolated cells include a small percentage of cells from other tissues of the medulla, which are systematically ignored during electrophysiological recordings. In this view, the RT-PCR data reported in Fig. 3 should be considered as a good qualitative support to the electrophysiological observations.

The cDNA was synthesized in a total volume of 50 μl with the High Capacity cDNA Archive kit (Applied Biosystems, Foster City, CA, USA). Polymerase chain reaction (PCR) experiments were carried out in a total volume of 25 μl, containing 2 μl of cDNA, 0.5 units of phusion high-fidelity DNA polymerase, 5× phusion GC buffer, 0.2% DMSO (Finnzymes, Finland), 0.2 mM of each deoxynucleotide triphosphate (Invitrogen, Carlsbad, CA, USA) and 0.5 μM specific primer set. The primer sequences used were: for α_{1H} (AF290213): 5′-GACGAGGATAAGACGTCT-3′ and 5′-AGGAGACG-CGTAGCCTGTT-3′; for α_{1G} (AF290212): 5′-TCAGAG-CCTGATTTCTTT-3′ and 5′-CAGGAGACGAAACCT-TGA-3′: for α_{1I} (AF290214): 5′-GATGAGGACCA-GAGCTCA-3′ and 5′-CAGGATCCGGAACTTGTT-3′; for α_{1E} (L15453): 5′-TAGTCTCGCCATCCTTTGAG-3′ and 5′-CCGATCACGGTAATGAAGTC-3′; for β-actin (NM_031144) 5′-GGACCTGACAGACTACCTCA-3′ and 5′-ATCTTGATCTTCATGGTGCT-3′; for DBH, dopamine β-hydroxylase (NM˙013158) 5′-CCTTGAA-GGGACTTTAGAGC-3′ and 5′-AGCAGCTGGTAG-TCCTGATG-3′. The non-saturated cycling conditions were 98°C for 30 s, followed by 26 cycles (for α_{1H}, α_{1G}, α_{1I}, β-actin and DBH) and 45 cycles (for α_{1E}) of 98°C for 15 s, 58°C for 30 s, and 72°C for 30 s. Experiments were

repeated at least 3 times for each primer. Positive controls (cDNA obtained from DNase-treated total RNA cortex of the same adrenal glands and from rat brain total RNA) and negative controls (water instead of template) were amplified in the same conditions. β-Actin was used as housekeeping gene to minimize intrinsic variation. The PCR product was run on 1% agarose gel stained with Gel Star (Cambrex Corporation, East Rutherford, NJ, USA) in the presence of a 100 bp DNA ladder as the molecular weight marker (Promega, Madison, WI, USA). To evaluate the variation of α_{1H}, α_{1E} and β-actin expression between control and hypoxia conditions we measured the band intensity using ImageJ 1.33u software (NHI, Bethesda, MD, USA). All samples were tested simultaneously for the different sets of primers.

Results

Ca^{2+} currents in normoxic RCCs

In a preliminary series of experiments we first tested for the presence of low-threshold Ca^{2+} currents in RCCs cultured in normoxic conditions (5% CO_2, 20% O_2), using the perforated-patch configuration and external solution containing (mM): 5 $CaCl_2$, 135 NaCl and 0 KCl. The zero KCl control conditions were set to hyperpolarize the resting cells and reduce steady-state T-type channel inactivation before clamping or applying KCl depolarizing solutions during amperometric measurements (see below). We found that, as previously reported (Cesetti *et al.* 2003), the present ionic conditions did not favour the expression of T-type channels, which were observed only in a small percentage of cells (22%). Most cells (78%, $n = 45$) exhibited high-voltage-activated (HVA) Ca^{2+} channels that started activating around -30 mV ($n = 39$ cells) and had weak inactivation during pulses of 100 ms and fast deactivating kinetics on return to -80 mV (Fig. 1*A*). Ramp commands exhibited *I–V* characteristics with a single peak at positive voltages (8.0 ± 0.7 mV, $n = 35$), suggesting a predominance of HVA channels (Fig. 1*B*). This was confirmed by the rapid kinetics of channel deactivation after a 20 ms pulse to -20 mV (Fig. 1*C*). Tail currents on repolarization to -100 or -50 mV were fast and monoexponential ($\tau_{fast} = 0.47 \pm 0.05$ at -100 mV and 0.56 ± 0.06 ms at -50 mV, $n = 22$ cells; inset in Fig. 1*C*), confirming that in most control RCCs Ca^{2+} currents were mainly carried by fast deactivating HVA channels.

Chronic hypoxia up-regulates α_{1H} T-type Ca^{2+} channels

In RCCs maintained under hypoxic conditions for 12–18 h (3% O_2, $n = 26$) cell capacitance was unmodified: 9.5 ± 0.6 pF and 10.8 ± 1.1 pF in control and hypoxic cells (Fig. 2*A*; $P < 0.27$), while membrane resting potential was significantly more positive after hypoxia. Current-clamp measurements in zero KCl solution gave mean resting potentials (V_{rest}) of -97.2 ± 3.5 mV ($n = 12$) in control RCCs and -76.2 ± 5.6 mV ($n = 10$; $P < 0.01$) in hypoxic cells, suggesting that, as in other cell preparations (Smirnov *et al.* 1994; Wyatt *et al.* 1995), CH reduces the resting K^+ channel permeability and/or increases a low-threshold Ca^{2+} conductance (see below).

In agreement with the observation of Del Toro *et al.* (2003) in PC12 cells, most of the hypoxic RCCs (85%) expressed T-type currents that started activating around -50 mV and displayed their characteristic fast inactivation during step depolarizations of 100 ms length (Fig. 2*A*). The hypoxia-recruited T-type channels produced a 'low-threshold shoulder' (second peak) around -24 mV in the *I–V* relationship (Fig. 2*C*), with mean current of 5.5 ± 0.5 pA pF^{-1} at -30 mV and exhibited a net increase of the quantity of charge from -50 to -20 mV, calculated as the time integral of the current during 100 ms depolarizations (Fig. 2*B*). A thorough analysis of

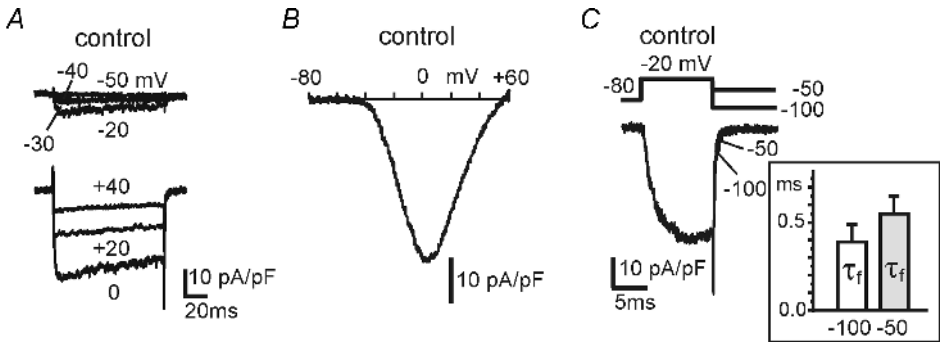

Figure 1. α_{1H} T-type channels are absent in adult RCCs but are expressed after CH
A, consecutive depolarizations at the potential indicated induce Ca^{2+} current which are visible starting from -30 mV and are weakly inactivating. *B*, a ramp command from -60 to $+60$ mV with a slope of 0.8 V s^{-1} produces a single inward current peak at $+5$ mV, indicating the absence of low-threshold channels. *C*, the kinetics of channel deactivation is fast at both -100 and -50 mV repolarizing voltages. Inset, time constants of tail currents (τ_f) at -100 and -50 mV obtained by fitting with an exponential decaying function.

the activation–inactivation parameters showed that the hypoxia-recruited T-type channels possess similar kinetic characteristics to the α_{1H} T-type channels expressed in cAMP-treated RCCs (Novara *et al.* 2004).

The existence of T-type channels was also confirmed by the slow deactivating tail current component at −50 mV following brief depolarizations to −20 mV (Fig. 2*E*). Tail currents of hypoxic RCCs were fast and monoexponential on returning to −100 mV ($\tau_{fast} = 0.4 \pm 0.08$ ms) and biexponentials at −50 mV with a fast and a slow component: $\tau_{fast} = 0.5 \pm 0.05$ and $\tau_{slow} = 6.5 \pm 0.8$ ms ($n = 11$) tails. The τ_{slow} value is in very good agreement with the reported deactivation time constant of rat brain α_{1H} subunit (McRory *et al.* 2001) and T-type channels of embryonic (Bournaud *et al.* 2001) and adult RCCs (Novara *et al.* 2004; see Discussion). Addition of 50 μM Ni^{2+} blocked the transient low-threshold currents during step depolarizations (Fig. 2*A*), the second peak during

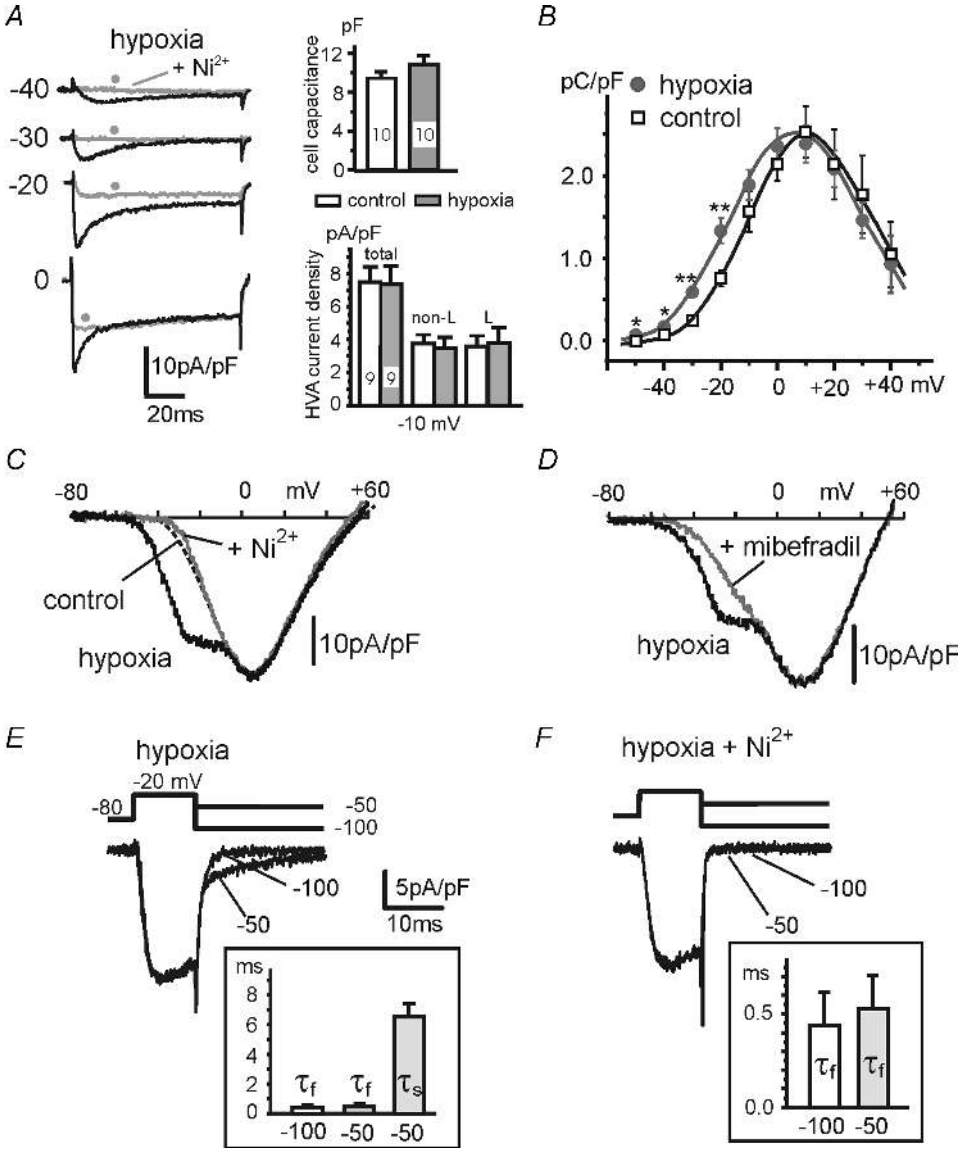

Figure 2. CH recruits α_{1H} T-type channels and preserves HVA current density
A, representative *I–V* traces from −40 to 0 mV after CH (dark traces) and addition of 50 μM Ni^{2+} (grey traces and filled circles). To the right are shown the cell capacitance values and the amplitude of current densities estimated before (total) and during application of 3 μM nifedipine (non-L) and their difference (L). *B*, mean quantity of charge *versus* voltage under control (open squares) and hypoxic conditions (filled circles) (*$P < 0.05$; **$P < 0.01$). *C* and *D*, hypoxic cells exhibit a double current peak during a ramp command. The 'low-threshold shoulder' is selectively abolished by 50 μM Ni^{2+} or mibefradil (1 μM). *E* and *F*, tail currents at −50 and −100 mV following a short depolarization to −20 mV. The tails at −50 mV have a slow deactivating component blocked by 50 μM Ni^{2+}. Insets, exponential fit with two time constants (τ_f and τ_s) for hypoxic cells at −50 mV and one time constant (τ_f) in hypoxia + Ni^{2+}.

ramp commands (Fig. 2*C*) and the slow tail during channel re-closure at −50 mV (Fig. 2*F*). Mibefradil (1 μM) was also very effective in blocking the low-threshold *I–V* component (Fig. 2*D*). Interestingly, as for PC12 cells (Del Toro *et al.* 2003), CH had no effects on the HVA current density and on the fraction of L- and non-L-type channels estimated at the end of a 100 ms pulse to −10 mV, during which T-type currents could fully inactivate (Fig. 2*A*, lower right panel). Percentage of L-type channels was $46.8 \pm 4.2\%$ in control and $52.4 \pm 4.1\%$ ($n = 9$; $P < 0.33$) in hypoxic cells, respectively. Taken together these findings support the view that CH selectively recruits a population of T-type channels of comparable density, kinetics and pharmacology to the α_{1H} channels recruited by long-term exposure to cAMP (Novara *et al.* 2004).

Chronic hypoxia selectively up-regulates the expression of α_{1H} T-type channels

Recruitment of α_{1H} during CH was also qualitatively supported by RT-PCR experiments performed on total RNA from isolated RCCs with primers against the α_{1H} subunit (see Methods). The expression level of α_{1H} subunit between control and hypoxic RCCs (16–18 h in 3% O_2) was compared by applying non-saturating PCR conditions. As control, we also used primers for DBH, a specific enzyme expressed by chromaffin cells, and for the housekeeping gene β-actin to evaluate RNA integrity. Semiquantitative RT-PCR analysis indicated that there is low-level expression of α_{1H} in normoxic cells and this is markedly increased after hypoxic treatment (1.7-fold; Fig. 3*A*). This agrees with the electrophysiological observation that a small percentage of control RCCs exhibited sizeable low-threshold currents (22%; see above). As a positive control we could confirm the presence of the α_{1H} subunit in cells isolated from the adrenal cortex (lane 5), which are known to express high densities of functional α_{1H} T-type channels (Schrier *et al.* 2001).

The selective action of hypoxia on α_{1H} was confirmed by semiquantitative RT-PCRs using primers against α_{1G} and α_{1I}, which revealed no messengers in control and hypoxic conditions, whereas positive controls using rat brains gave the expected products (Fig. 3*B*). In order to exclude a contribution of R-type (Cav2.3) Ca^{2+} channels in the recruitment of low-threshold currents and secretion in hypoxic conditions, we also tested the α_{1E} expression level in RCCs by RT-PCR. In Fig. 3*C* it is shown that the α_{1E} subunit is weakly expressed both in normal and hypoxic cells without any significant increase after the treatment. The basal low-level of α_{1E} expression in the medulla required a high number of PCR cycles to be revealed and compared with β-actin expression (see Methods).

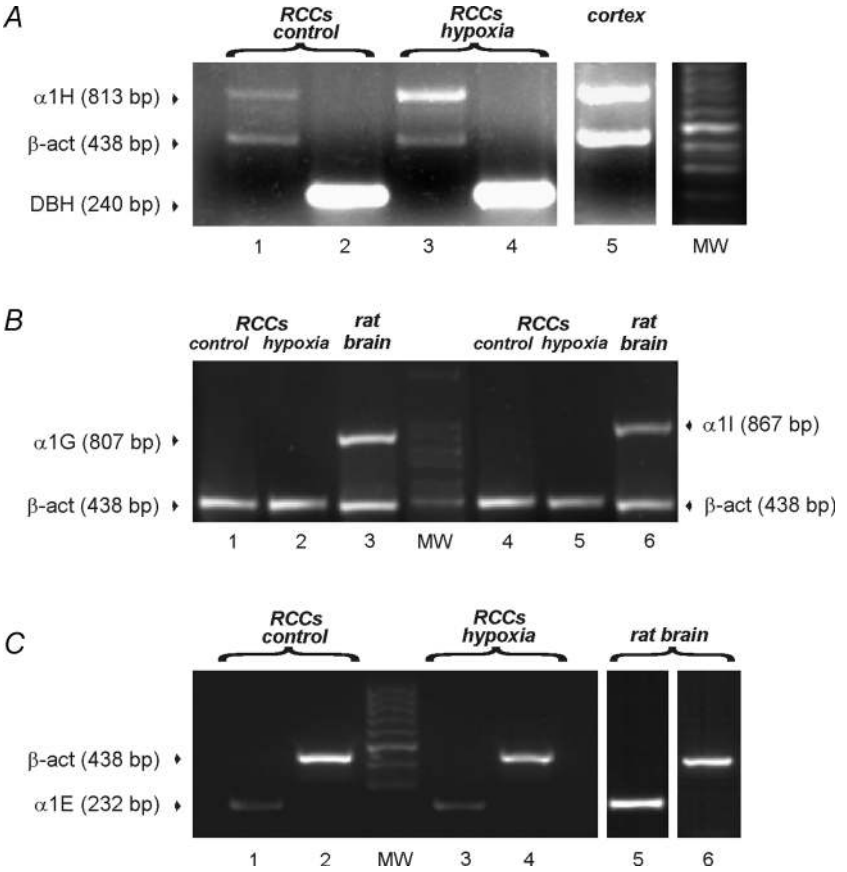

Figure 3. Selective increased expression of α_{1H} subunit mRNA in hypoxia-treated RCCs from the medulla
Total RNA from RCCs of the adrenal medulla of adult rats was retrotranscribed and amplified with specific oligonucleotides (0.5 μM) for α_{1H}, α_{1G}, α_{1I}, α_{1E}, DBH and β-actin. *A*, enhanced expression of α_{1H} subunit after incubation in hypoxic condition (16–18 h with 3% O_2). PCR products for α_{1H} plus β-actin (lanes 1, 3 and 5) and for DBH (lanes 2 and 4). Untreated RCCs are in lanes 1 and 2 and hypoxia-treated RCCs in lanes 3 and 4. The mRNA of the adrenal cortex isolated cells is used as a positive control (lane 5). *B*, the α_{1G} and α_{1I} subunits are not expressed in control and hypoxia-treated RCCs. The PCR products for α_{1G} plus β-actin (lanes 1, 2 and 3) and for α_{1I} plus β-actin (lanes 4, 5 and 6) are shown in control cells (lanes 1 and 4) and in hypoxia-treated RCCs (lanes 2 and 4). Positive control for the reaction is the mRNA from the entire rat brain (lanes 3 and 6). *C*, the α_{1E} subunit is weakly expressed and not further up-regulated after hypoxic treatment in RCCs. PCR products for α_{1E} (lanes 1, 3 and 5) and for β-actin (lanes 2, 4 and 6). Normoxic cells are in lanes 1 and 2 and hypoxic RCCs in lanes 3 and 4. The mRNA from rat brain is used as positive control (lanes 5 and 6). PCR products were separated in 1% agarose gel in the presence of 100 bp DNA ladder (lane MW). Experiments were repeated at least 3 times for each primer.

T-type channel recruitment requires HIF activation and occurs regardless of extracellular Ca^{2+}

The iron chelator DFX is commonly used as a hypoxia-mimicking factor since it inhibits the prolyl-hydroxylases that stimulate the proteasomal degradation of HIF1-α and HIF2-α. Thus, in order to test whether T-type channel recruitment proceeds through the activation of HIF, RCCs were treated with DFX. As shown in Fig. 4, overnight incubation with DFX (12–18 h, 300 μM) induced marked up-regulation of T-type channels in RCCs similar to CH. In particular, DFX produced (1) the typical low-threshold fast inactivating Ca^{2+} currents at −50 to −30 mV observed in 70% of DFX-treated cells (Fig. 4*A*), (2) a net increase of the quantity of charge below −20 mV (Fig. 4*B*; $n = 16$), (3) a 'low-threshold shoulder' at -20 ± 2.2 mV followed by a major peak at 8.6 ± 2.4 mV (Fig. 4*C*), and (4) delayed tail currents on repolarization to −50 mV (Fig. 4*D*). Similar effects were also observed with lower doses of DFX (150 μM). Thus, HIFs appear to be involved in gene expression of T-type channels during CH.

Next, we tested whether enhanced cytosolic Ca^{2+} levels that usually accompany cell responses to hypoxia could be also involved in this process. Indeed, reduced P_{O_2} levels activate Ca^{2+}-dependent protein kinases and phosphatases and removal of extracellular Ca^{2+} abolishes hypoxic accumulation of HIF-2α, preventing gene expression and cell remodelling (Seta *et al.* 2004). To test the role of external Ca^{2+}, we performed a series of experiments keeping control, hypoxic and DFX-treated cells in a modified DMEM deprived of Ca^{2+}. We found that even in the absence of Ca^{2+} in the culture medium, T-type currents were still present in both hypoxic and DFX-treated cells (data not shown). Ca^{2+} currents between −50 mV and −20 mV were fast and fully inactivating and had delayed tail currents on return to −50 mV, similar to those illustrated in Figs 2 and 4. Under commands, the Ca^{2+} currents displayed the typical low-threshold shoulder around −20 mV.

T-type channel recruitment by hypoxia or DFX is independent of PKA activation

Long-term exposures to cAMP produce a marked increase of T-type currents in RCCs through a cAMP-dependent PKA-independent pathway that involves Epac cAMP-receptor proteins (Novara *et al.* 2004). Since CH causes up-regulation of cAMP and activation of PKA-dependent processes in various cell preparations (Seta *et al.* 2004), we tested whether a cAMP–PKA pathway could mediate the recruitment of T-type channels during CH, by using the PKA inhibitor H89 and the competitive antagonist Rp-cAMPs.

As shown in Fig. 5, overnight incubation of H89 (1 μM) in the culture medium had no effects on the expression of T-type channels in hypoxic cells. Fast inactivating T-type currents from −50 to −20 mV were observed in most of the hypoxic cells preincubated with H89 (Fig. 5*A*) and the *I–V* characteristics during ramp commands showed a 'low-threshold shoulder' at -23 ± 1.3 mV in 71% of cells (Fig. 5*B*). The total Ca^{2+} charge entering at potentials below −20 mV showed a net increase ($n = 24$) (Fig. 5*C*) and tail currents had a prominent delayed component in most RCCs (85%; $n = 13$). Tail currents were fitted by a single exponential function at −100 mV ($\tau_{fast} = 0.6 \pm 0.1$ ms) and by two exponentials at −50 mV ($\tau_{fast} = 0.44 \pm 0.06$ ms, $\tau_{slow} = 6.41 \pm 0.83$ ms). Similar conclusions could be achieved by comparing DFX- and DFX + H89-treated cells (Fig. 5*E*). In the latter case, 77% of the cells tested exhibited slow re-closures at −50 mV ($\tau_{fast} = 0.59 \pm 0.06$ ms, $\tau_{slow} = 9.35 \pm 2.1$ ms; $n = 22$). T-type channel up-regulation following CH was also evident in the presence of 1 μM Rp-cAMPs, the competitive antagonist of cAMP for binding to PKA. Figure 6 summarizes the results obtained in 85% of the 14 cells tested, which are similar to those of Fig. 5. In conclusion, it appears that the hypoxia-induced recruitment of T-type channels proceeds regardless of PKA activation.

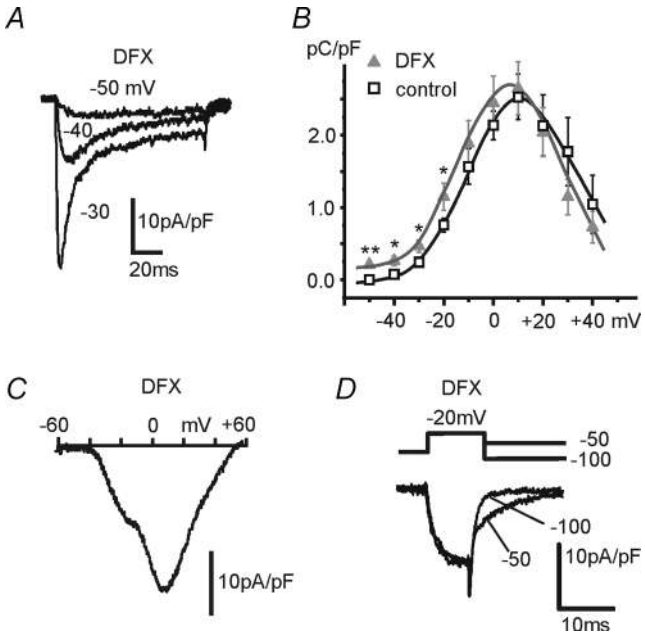

Figure 4. Overnight incubations with DFX induce T-type channel recruitment
A, transient T-type Ca^{2+} currents recorded at the potentials indicated from an RCC incubated overnight with 300 μM DFX. *B*, mean charge densities in control (open squares) and DFX-treated cells (filled triangles) at different voltages (*$P < 0.05$; **$P < 0.01$). *C*, typical *I–V* characteristics with a clear 'low-threshold shoulder' recorded from a DFX-treated cell during a ramp command. *D*, tail currents at −50 and −100 mV from a cell treated with DFX.

Hypoxia- and DFX-recruited T-type channels contribute to 'low-threshold' secretion

cAMP-recruited T-type channels contribute to low-threshold exocytosis that is usually absent in control RCCs (Giancippoli *et al.* 2006). In addition, CH recruits a Cd^{2+}-insensitive secretory activity in PC12 cells attributed to Ca^{2+} flowing through non-voltage-gated Ca^{2+} channels (Taylor *et al.* 1999). Therefore, we thought it interesting to test whether hypoxia- and DFX-recruited T-type channels contribute to secretion as cAMP-recruited T-type channels and if this Ca^{2+}-dependent mechanism is the main one responsible for 'low-threshold secretion' in hypoxic RCCs.

Exocytosis in hypoxic and DFX-treated cells was already evident at −50 mV and was significantly different from controls between −50 and −20 mV (Fig. 7*A* and *B*, $n = 26$ hypoxic, $n = 16$ DFX treated). A capacitance change (ΔC) of about 18 fF at −30 mV was observed after hypoxic stimulation (Fig. 7*C*) and about half of it was associated with the T-type channels expressed in hypoxic cells. We also checked whether TEA^+ ions in the external medium could bias our findings. We replaced TEA^+ with Na^+ ions and added 300 nM TTX to block voltage-gated Na^+ currents. In this case, the averaged ΔC value after depolarization was calculated over a 500 ms window, excluding the first 70 ms to avoid non-secretory capacitive transients associated with the slow-down of Na^+ gating currents induced by TTX (Horrigan & Bookman, 1994). As shown in Fig. 7*D*, replacement of TEA^+ with Na^+ does not produce any major changes to the secretory responses of control and hypoxic RCCs, confirming that α_{1H} T-type channels recruited by CH and DFX treatment are functionally coupled to the secretory apparatus of RCCs.

In order to compare the secretory responses of hypoxic and DFX-treated cells with those induced by pCPT-cAMP, we used the same experimental conditions which have been previously employed (Giancippoli *et al.* 2006). N-, P/Q- and L-type channels were blocked by incubating the cells with ω-CTx-GVIA (3.2 μM) plus ω-Aga-IVA (2 μM) and adding nifedipine (1 μM) to the bath. The external solution contained 145 mM TEACl and 5 mM $CaCl_2$ to minimize Na^+ inward currents without using TTX (see Methods). Under these conditions, contribution to secretion was limited to toxin-resistant R-type and T-type channels, when expressed (Fig. 7*A* and *B*). As for the ΔC associated with the cAMP-recruited T-type channels, also the capacitance change evoked during low-threshold pulses in hypoxic conditions was fully blocked by 50 μM Ni^{2+} (Fig. 7*E*). This suggests that Ni^{2+}-sensitive T-type channels are the main channels responsible for the

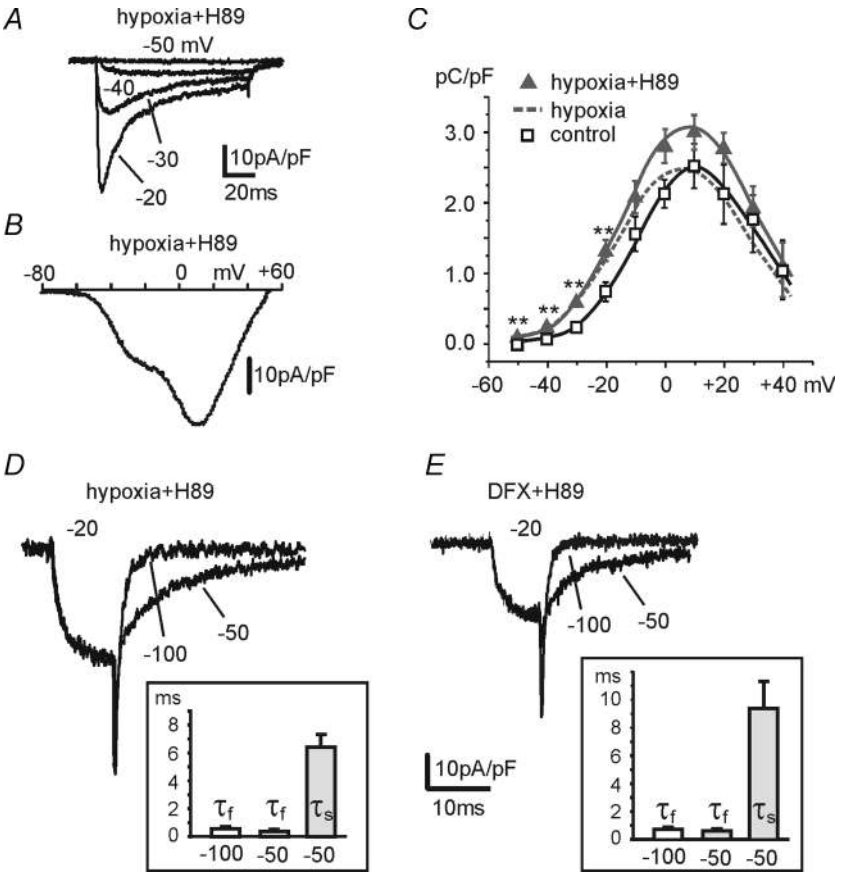

Figure 5. PKA is not involved in hypoxia-induced T-type channel recruitment
Overnight incubation with the PKA inhibitor H89 (1 μM) did not perturb the recruitment of T-type channels by CH. *A*, representative T-type currents recorded at the indicated potentials from an RCC incubated overnight with H89 in CH. *B*, *I–V* characteristics recorded with a ramp command from the same cell as in *A*. *C*, mean charge densities *versus* voltage (100 ms depolarizations) for hypoxic, hypoxic + H89 and control cells (**$P < 0.01$). *D* and *E*, slow tails at −50 mV in hypoxic or DFX-treated cells are still evident in the presence of H89. Same pulse protocol as in Fig. 4D. Insets, mean values of the decaying exponential time constants.

hypoxia-recruited 'low-threshold' secretion. Notice also that at variance from the recordings of Fig. 7*A* and *B* the $\Delta C(V)$ data of Fig. 7*C* and *D* are derived from cells that were not treated with ω-toxins and nifedipine. Thus, secretion in these cells was induced by T-type and all the available HVA channels.

It is also worth noticing that DFX potentiation of α_{1H} T-type currents and the associated secretory responses (Fig. 8*A*) have comparable amplitudes and similar voltage dependence to those measured during exposures to pCPT-cAMP (Fig. 8*B* and *C*), supporting the view that the two distinct pathways (HIF and cAMP) potentiate low-voltage exocytosis by selectively recruiting the same Ca^{2+} channel subunit.

Hypoxia-recruited T-type channels induce exocytotic bursts during mild KCl depolarizations

Exocytosis of single chromaffin granules, associated with Ca^{2+} entry through hypoxia-recruited T-type channels, was investigated by measuring the amperometric spikes evoked by cell depolarizations with 2–15 mM extracellular KCl, 10 mM $CaCl_2$ and 3 μM nifedipine to block the contribution of L-type channels. The inset of Fig. 9*A* shows mean values of resting potentials (V_{rest}) *versus* [KCl] in perforated-patch conditions obtained with ionic solutions similar to those used for the amperometric detections. As can be noticed, hypoxic cells were more depolarized in 0 mM KCl (−76 mV *versus* −97 mV), but V_{rest} approached closer values as [KCl] was raised to 15 mM (−31 mV and −45 mV; dashed lines). The thick continuous lines in the inset are theoretical curves predicted by the Goldman–Hodgkin–Katz equation assuming that only K^+, Na^+ and Ca^{2+} channels contribute to V_{rest}, with permeability ratios of $P_{Na}/P_K = 0.01$ and $P_{Ca}/P_K = 0.01$ in control and $P_{Na}/P_K = 0.015$ and $P_{Ca}/P_K = 0.02$ in hypoxic cells (see Fig. 9*A* legend). This accounts for a possible reduced K^+ channel density in hypoxic conditions as reported in other cells (Smirnov *et al.* 1994; Wyatt *et al.* 1995; Wang *et al.* 1997) and for an increased stationary T-type conductance as shown below.

Increasing extracellular [KCl] caused progressive increases of the frequency of exocytotic bursts (Fig. 9). Under normoxic conditions, amperometric spikes were absent or rare in 2 mM ($n = 20$) or 4 mM $[KCl]_o$ ($n = 18$) (mean frequency < 0.04 Hz). On the contrary, when the same solutions were applied to hypoxic cells, the mean frequency of amperometric spikes was significantly different from controls: 0.12 Hz in 2 mM KCl ($n = 26$, $P < 0.05$) that increased to 0.15 Hz in 4 mM KCl ($n = 21$, $P < 0.05$) (inset in Fig. 9*B*). This was expected since in control conditions the only HVA channels available are mainly closed between −75 and −60 mV in 2 and 4 mM KCl, while in hypoxic cells the expressed

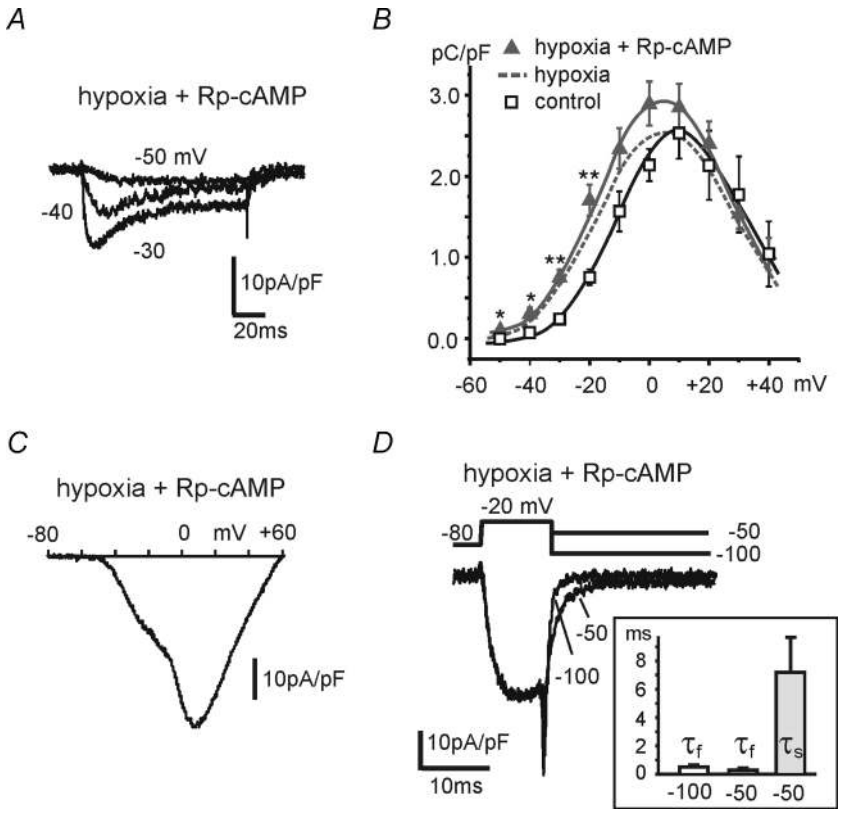

Figure 6. The cAMP antagonist Rp-cAMP does not prevent T-type channel recruitment by hypoxia
A–D, T-type currents, *I–V* characteristics, mean charge densities and tail currents recorded with the same protocols of Figs 4 and 5 from hypoxic RCCs incubated with the cAMP antagonist Rp-cAMP (1 μM) (*$P < 0.05$; **$P < 0.01$).

T-type channels are partially open between −63 and −54 mV. Spike frequencies in normoxic and hypoxic RCCs converge to higher values when $[KCl]_o$ is raised to 10 mM (0.21 ± 0.05 Hz for controls, $n = 24$ and 0.27 ± 0.05 for hypoxic cells, $n = 14$) and V_{rest} is increased to −45 and −41 mV, respectively.

Additional evidence that amperometric spikes during mild depolarizations are evoked by Ca^{2+} influx through T-type channels was obtained by blocking their activity with 50 μM $NiCl_2$. In these experiments, control and hypoxic cells were pretreated with ω-CTx GVIA, ω-Aga IVA and nifedipine to block L-, N- and P/Q-type channels. Figure 9*C* and *D* shows that in normoxic conditions the mean frequency of exocytotic bursts in 15 mM [KCl] was not significantly different after adding 50 μM Ni^{2+} ($P < 0.5$), while the same blocker reduced to nearly one-third of control values the mean frequency in hypoxic RCCs (Fig. 9*D* and *E*).

Further support for the presence of a steady T-type channel contribution to secretion in 2–4 mM KCl came from testing the action of 50 μM Ni^{2+} on V_{rest} and membrane conductance (R_m). We found that Ni^{2+} did not alter the mild depolarization and partial decrease of R_m induced by 4 mM KCl in control cells ($n = 5$) (Fig. 10*A*), while producing a partial hyperpolarization of 6.5 ± 0.5 mV ($n = 5$) and a small significant increase of R_m

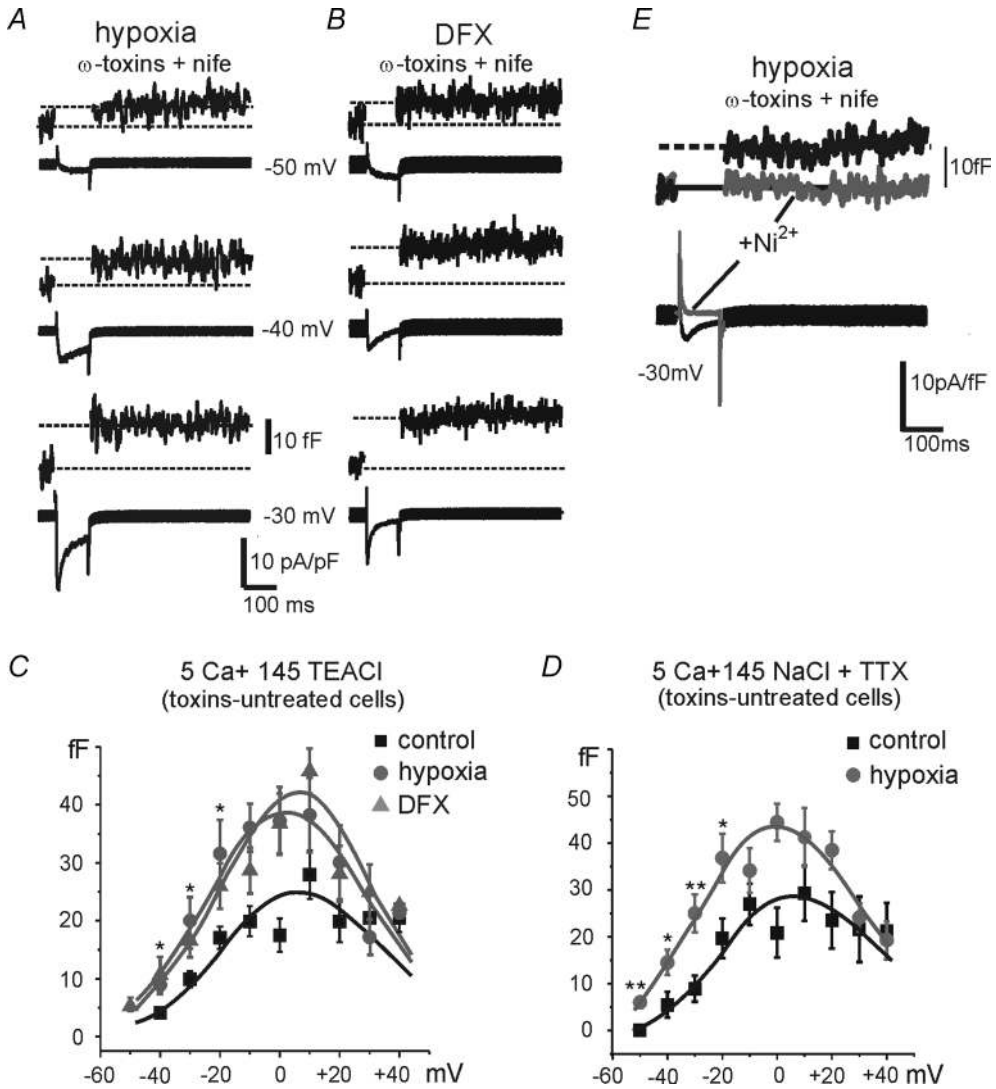

Figure 7. Depolarization-evoked secretion in hypoxic and DFX-treated cells
A and *B*, representative Ca^{2+} currents and depolarization-evoked secretory responses for a hypoxic and DFX-treated cell in the presence of ω-toxins and nifedipine. *C* and *D*, capacitance changes (ΔC) *versus* voltages for control, hypoxic and DFX-treated cells, measured in 5 mM Ca^{2+} and 145 mM TEACl (*C*) or 145 mM NaCl + 0.3 μM TTX (*D*) (*$P < 0.05$; **$P < 0.01$). *E*, Ca^{2+} currents and capacitance changes in the presence of ω-toxins and nifedipine at −30 mV from a hypoxic RCC before and during application of 50 μM Ni^{2+}.

(from 0.63 ± 0.1 GΩ to 0.71 ± 0.1 GΩ ($n = 4$); $P < 0{,}05$) in hypoxic RCCs (Fig. 10*B*). This indicates that T-type channels produce a steady 'window current' contributing to the partial cell depolarization and catecholamine release near resting hypoxic conditions. We also found that hypoxia increased R_m with respect to control RCCs from 1.8 ± 0.3 GΩ ($n = 8$) to 2.9 ± 0.4 GΩ ($n = 4$) ($P < 0.05$) in 0 KCl as expected from a reduction of available K^+ channels (Smirnov *et al.* 1994). The transient time course of the Ni^{2+}-induced hyperpolarization in Fig. 10*B* is most likely due to the closing of Ca^{2+}-dependent SK channels which are expressed in RCCs and require low $[Ca^{2+}]_i$ to activate near resting potentials (Neely & Lingle, 1992). Closing of SK channels may derive from the slow clearing of cytosolic Ca^{2+} by intracellular organelles (Park *et al.* 1996) following T-type channel block.

Hypoxia does not alter the time course and size of single amperometric spikes

To complete the analysis and test whether hypoxia affects the kinetics of secretion we compared the parameters characterizing the time course and size of amperometric spikes (Machado *et al.* 2001) in control and hypoxic cells. As shown in the insets of Fig. 9*C* and *E*, hypoxia does not alter the time course of spikes recorded before and during Ni^{2+} application. The two spikes of Figs 9*C* (1 and 2) perfectly overlap during the rising and falling phase. An accurate analysis of the rise time (t_m), time to peak (t_p) and spike width at half the peak amplitude ($t_{1/2}$) indicates that they are comparable in control and hypoxia conditions and the same is true for the maximal amplitude of the spike (I_{max}) and the total quantity of charge released (Q) (Fig. 10*C*). This suggests that CH and recruitment of T-type channels do not alter the biophysical parameters that characterize vesicle content and speed of catecholamine release during exocytosis.

Discussion

We provided evidence that 12–18 h of CH causes a net recruitment of T-type channels that are weakly or not expressed in normoxic RCCs. The effect is specific for low-voltage-activated Ca^{2+} currents and resembles closely the slow action mediated by the cAMP/Epac pathway, which recruits comparable densities of T-type channels (Novara *et al.* 2004) and produces comparable capacitance changes associated with vesicle fusion and secretion (Giancippoli *et al.* 2006). Our data show clearly that hypoxic RCCs secrete catecholamines at rest, near physiological conditions (2–4 mM KCl). The 'low-threshold' exocytotic bursts in this case have a frequency significantly higher than in normoxic cells, last several minutes and are mainly controlled by a small fraction (1–2%) of T-type channels already open at resting potentials. This suggests that cell depolarizations induced by CH cannot be attributed only to a decreased K^+ permeability (Smirnov *et al.* 1994; Wyatt *et al.* 1995; Wang *et al.* 1997) but also involve an increased T-type conductance that lowers membrane resistance and induces basal release of catecholamines near resting conditions.

Our patch-clamp recordings show clearly that the hypoxia-regulated T-type channel is the α_{1H} isoform. The T-type current has fast kinetics of activation and deactivation that are common to α_{1G} and α_{1H} and high sensitivity to Ni^{2+} that is typical of α_{1H} (Lee *et al.* 1999; Novara *et al.* 2004). The estimated 6.5 ms deactivation time constant (τ_{slow}) at −50 mV in hypoxic conditions is in good agreement with the extrapolated value of τ_{deact} (6.7 ms) of rat brain α_{1H} at −65 mV in 2 mM Ca^{2+} and whole-cell recording conditions (McRory *et al.* 2001) if a −15 mV shift is allowed to compensate for the liquid-junction potential of our recording conditions (5 mM Ca^{2+} and perforated-patches). Similar values are also reported for the α_{1H} T-type channels of embryonic (6.2 ms at −50 mV in 10 mM Ba^{2+} and whole-cell recordings; Bournaud *et al.* 2001) and adult RCCs (5.8 ms at −45 mV in 10 mM Ca^{2+} and whole-cell recording conditions; Novara *et al.* 2004).

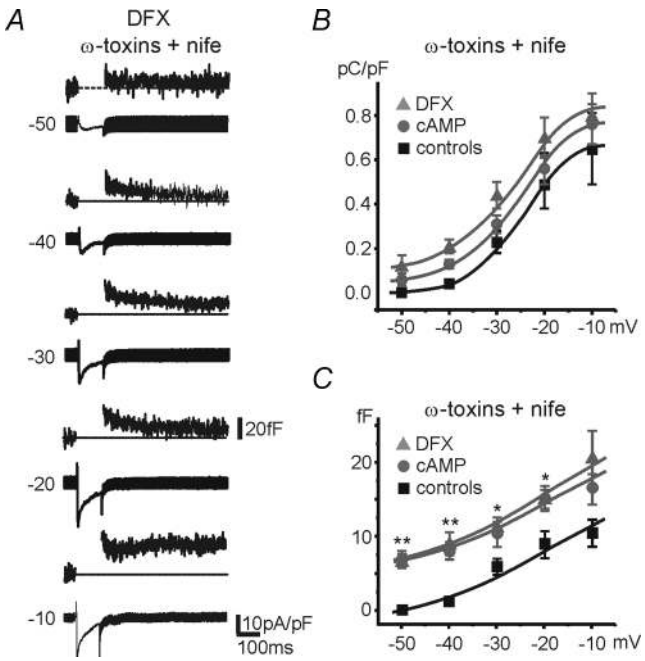

Figure 8. Comparative effects of DFX and pCPT-cAMP on 'low-threshold' secretion
A, representative Ca^{2+} currents and depolarization-evoked secretory responses for a DFX-treated cell at the potentials indicated. L-, N- and P/Q-type channels were blocked by ω-toxins and nifedipine. *B* and *C*, mean charge densities (pA pC^{-1}) and capacitance changes (fF) *versus* voltages for control, DFX- and pCPT-cAMP-treated cells, measured in 5 mM Ca^{2+} and 145 mM TEA-Cl. Data with pCPT-cAMP were taken from Giancippoli *et al.* (2006) (*$P < 0.05$; **$P < 0.01$).

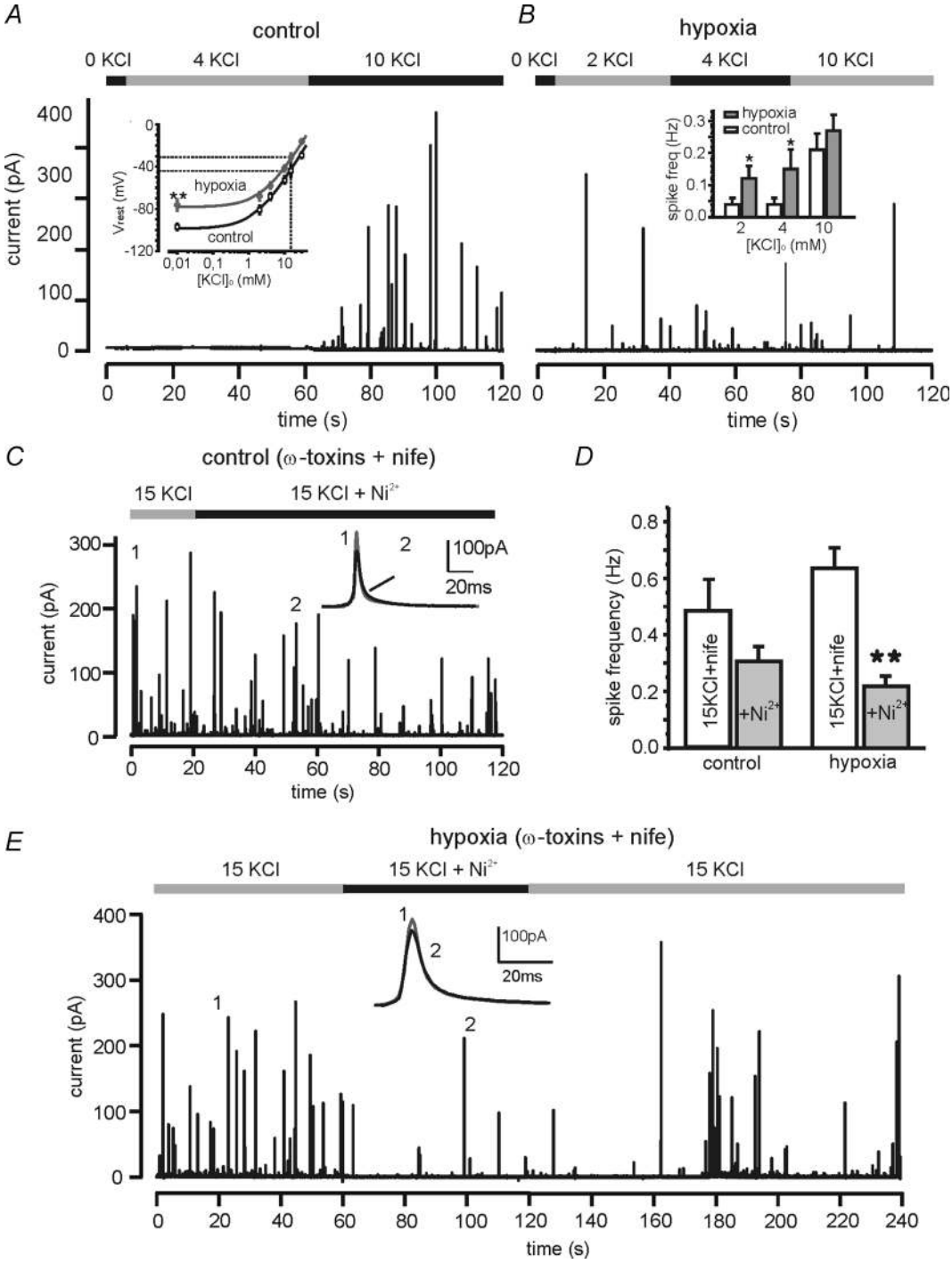

Figure 9. Amperometric spikes evoked by mild KCl depolarizations under normoxic and hypoxic conditions

A, amperometric spikes recorded from a control RCC exposed to 0, 4 and 10 mM KCl solutions as indicated by the bars. Spikes were visible only when 10 mM KCl solutions were applied. Inset, mean resting potentials *versus* $[KCl]_o$ for control cells. Data points were obtained from $n = 12$–4 (the number of cells n changes from 4 to 12 at every potential) cells for each concentration (**$P < 0.01$). The two continuous curves were calculated from the Goldman–Hodgkin–Katz (GHK) equation derived by Jan & Jan (1976) and Lewis (1979). Permeability ratio was $P_{Na}/P_K = 0.01$ and $P_{Ca}/P_K = 0.01$ in control and $P_{Na}/P_K = 0.015$ and $P_{Ca}/P_K = 0.02$ in hypoxic conditions. Ion concentrations were (mM): $[K^+]_i = 140$, $[Na^+]_i = 140$, $[Ca^{2+}]_i = 0.0001$, $[Na^+]_o = 135$ and $[Ca^{2+}]_o = 10$. The two theoretical curves were shifted vertically by +12 mV to account for the liquid junction potential of our perforated-patch recording conditions. The curve matching the data of hypoxic cells was further shifted by +10.5 mV to compensate for either a changed surface charge potential or altered

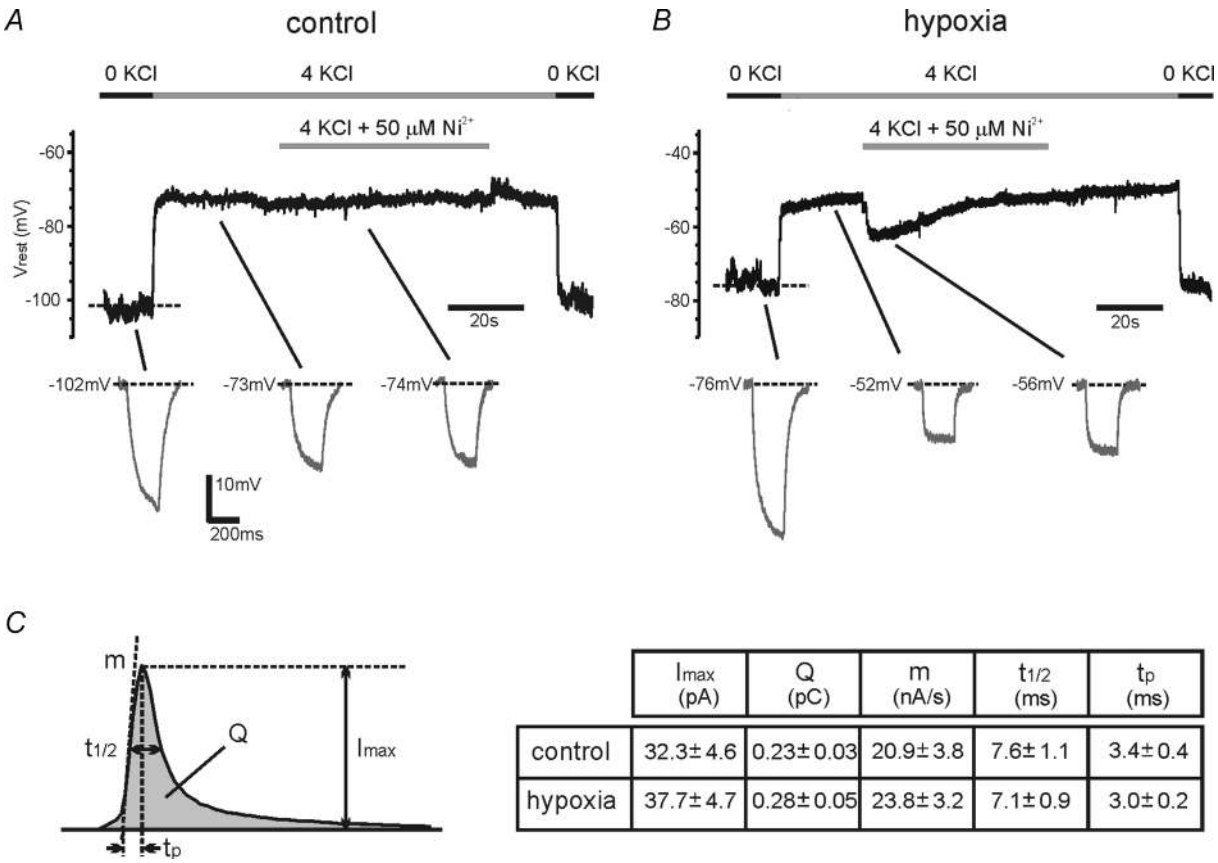

	Imax (pA)	Q (pC)	m (nA/s)	t1/2 (ms)	tp (ms)
control	32.3±4.6	0.23±0.03	20.9±3.8	7.6±1.1	3.4±0.4
hypoxia	37.7±4.7	0.28±0.05	23.8±3.2	7.1±0.9	3.0±0.2

Figure 10. Hypoxia lowers the RCC resting potential and uncovers a T-type channel contribution blocked by 50 μM Ni^{2+}

A and *B*, resting potentials (V_{rest}) and membrane resistance (R_m) measurements in current-clamp mode in control and hypoxic RCCs in the ionic conditions indicated. R_m was estimated using 20 pA hyperpolarizing pulses of 200 ms. In *A* the cell is more hyperpolarized than in hypoxic conditions and 4 mM KCl causes a 30 mV depolarization and decreases R_m. Addition of 50 μM Ni^{2+} caused no changes to both V_{rest} and R_m. In *B* the hypoxic cell is more depolarized and has higher R_m in 0 mM KCl. In 4 mM KCl, both V_{rest} and R_m decrease and addition of 50 μM Ni^{2+} produces a 9 mV transient hyperpolarization followed by an increased R_m as expected from the block of an inward T-type 'window-current'. *C*, effects of hypoxia on the secretory spike parameters from amperometric recordings similar to those shown in Fig. 9*C* and *E*. All the used parameters are indicated on the representative amperometric event to the left (see text for their definition).

The agreement is even more impressive if comparing the asymptotic values of τ_{deact} at -110 mV for the three channels, which are unaffected by the voltage shifts of different ionic conditions: 1.4 ms (McRory *et al.* 2001), 1.3 ms (Bournaud *et al.* 2001) and 1.0 ms (Novara *et al.* 2004).

The selective up-regulation of α_{1H} is also nicely supported by the RT-PCR data, which show that α_{1H} is the only Ca_v3 channel isoform recruited by hypoxia. In agreement with the electrophysiological data of Fig. 2*A* we can also exclude the involvement of R-type channels, as the $Ca_v2.3$ (α_{1E}) isoform is weakly expressed in RCCs and is

Na^+/Ca^{2+} transport causing slight depolarization if activated by the increased activity induced by Ca^{2+} entry through hypoxia-recruited T-type channels (Sjodin, 1980). *B*, amperometric spikes recorded from a hypoxic RCC exposed to different KCl solutions as indicated. Cells were more depolarized with respect to control in 0 KCl and events were already visible with 2 mM KCl solutions. Inset, mean frequency of amperometric spikes in control and hypoxic conditions calculated from a variable number of cells (*$P < 0.05$). *C* and *E*, amperometric spikes evoked by 15 mM KCl + 1 μM nifedipine, before (grey bar) and during 50 μM Ni^{2+} addition (black bar) in control and hypoxic RCCs. All experiments were performed after ω-toxin incubation. In the insets are shown the time course of the indicated amperometric events at a more expanded time scale. Notice the reversible action of Ni^{2+} in the hypoxic cell. *D*, the T-type channel blocker had no effect on the mean frequency of bursts in control RCCs, whereas it significantly reduced the mean frequency of hypoxic cells (**$P < 0.01$).

not up-regulated during hypoxia. R-type channels can be confused with T-type channels for their fast inactivating time course and sensitivity to Ni^{2+} and, thus, could have been easily overlooked in our voltage-clamp recordings. However, the negative results of the RT-PCR would exclude this possibility.

We found it interesting that CH- or cAMP-treated RCCs up-regulate the α_{1H} channel isoform that is highly expressed in the adrenal glomerulosa of adult rats but not in the chromaffin cells of the medulla (Schrier *et al.* 2001). The absence of T-type channels in RCCs seems, however, to be a critical issue linked to the developmental stage of the adrenal gland. In fact, T-type α_{1H} channels are already expressed in immature RCCs at the embryonic stage (although not coupled to secretion; Bournaud *et al.* 2001), in RCCs of neonatal rats (K. I. Levitsky & J. Lopez-Barneo, personal communication) and in a small percentage of adult RCCs (Hollins & Ikeda, 1996; Novara *et al.* 2004). Thus, it seems that development causes down-regulation of α_{1H} channels which can be readily reversed following long-lasting stressful conditions (see Carbone *et al.* 2006).

Ca^{2+} channels remodelling during chronic hypoxia

CH acts at the transcriptional level, altering expression of numerous proteins and inducing remodelling of ion channel distributions in O_2-sensitive cells (Montoro *et al.* 1996). A common response to CH is the down-regulation of Kv channels that causes cell depolarization, Ca^{2+} channel openings and increased intracellular Ca^{2+} (Seta *et al.* 2004). Also voltage-gated Ca^{2+} channels participate in the cell response to CH, although their redistribution appears heterogeneous and depends on cell types and hypoxic conditions. In most cases the effects are limited to an up-regulation of L-type channels in PC12 and carotid body glomus cells (Hempleman, 1996; Scragg *et al.* 2005), while their density is partially reduced in cardiac hypertrophied right-ventricular cells (Chouabe *et al.* 1997). These effects, however, are variable and linked to the way hypoxia is induced (directly on animals or on isolated cultured cells) and to the percentage of O_2 reduction (3–10% O_2). In fact, the L-type channel density remains unaltered in PC12 cells exposed to 3% O_2 for 24 h (Del Toro *et al.* 2003), in carotid body glomus cells isolated and cultured in 6% O_2 for 1–2 weeks (Stea *et al.* 1995) and in adult RCCs, as shown in Fig. 2*A*. All this suggests some caution in drawing general conclusions on the role of voltage-gated Ca^{2+} channels in CH.

CH seems particularly effective in recruiting α_{1H} T-type channels in PC12 cells (Del Toro *et al.* 2003) and RCCs. Recruitment of α_{1H} channels appears compatible with low P_{O_2} conditions since their current amplitude is only partially inhibited by acute hypoxia ($< 14\%$) when expressed in HEK-293 cells (Fearon *et al.* 2000). Our data allow also a rough estimate of the amount of T-type channels expressed and of the size of 'window-current' available at resting potentials where basal secretion of catecholamine occurs. Since block of T-type channels causes a mean resting hyperpolarization of about 5 mV (Fig. 10*B*), the steady T-type inward current responsible for this potential drop across a membrane resistance of 0.6 GΩ is about 8 pA. This value is relatively large due to the high extracellular Ca^{2+} (10 mM) but is in good agreement with values of T-type 'window currents' reported in myotubes (3 pA in 2 mM Ca^{2+}; Bijlenga *et al.* 2000) and central neurons (15–20 pA in 2 mM Ca^{2+}; Crunelli *et al.* 2005) in which the T-type 'window current' plays key roles in myoblast differentiation and oscillatory firing behaviours in central neurons. Notice that a steady inward current of several picoamps can be derived by multiplying the percentage of T-type channels steadily open at −50 mV (p) by the total number of expressed T-type channels (N), the single channel conductance (γ) and the driving force ($V–E_{Ca}$). In our case, with $p = 2\%$ (derived from the overlapping of the activation and inactivation curves; Novara *et al.* 2004), $N = 2800$ channels (assuming a channel density of 4 channels μm^{-2} and a cell diameter of 15 μm; Giancippoli *et al.* 2006), $\gamma = 2.5$ pS in 10 mM Ca^{2+} (Carbone & Lux, 1987) and $V–E_{Ca} = -120$ mV we obtain a 'window current' of 17 pA.

It is also interesting to underline that an inward Ca^{2+} current of 17 pA carries a total charge of 1.7 pC within 100 ms that corresponds to the quantity of charge injected during a step depolarization of 100 ms to −50 mV (Fig. 8*B*). This amount of charge induces 7 fF capacitance change corresponding to the fusion of seven vesicles (Tabares *et al.* 2001). Therefore, the estimated T-type 'window current' in hypoxic cells can well account for both the more positive resting potentials and the sustained 'low-threshold' exocytosis near resting conditions.

Hypoxia-recruited T-type channels are functionally coupled to low-threshold exocytosis

T-type channels are effectively coupled to neurotransmitter secretion in a number of cell preparations including invertebrate neurons, retinal bipolar cells, olfactory bulbs and chromaffin cells (see Carbone *et al.* 2006). Thus, it is not surprising that hypoxia-recruited T-type channels are coupled to catecholamine release with a Ca^{2+} efficiency that is comparable to that of α_{1H} channels recruited by Epac and fully blocked by Ni^{2+} (Giancippoli *et al.* 2006). This excludes a hypoxia-induced potentiation of exocytosis mediated by Ca^{2+}-permeable pathways as in the case of PC12 cells in which CH induces an increased secretion via formation of amyloid β-peptide permeable to Ca^{2+} and insensitive to Cd^{2+} (Green *et al.* 2002). Figure 8 shows clearly that the three treatments (hypoxia, DFX and cAMP) produce capacitance increases of 7–10 f F associated with a Ca^{2+} entry that is almost constant

above −40 mV. This peculiarity causes a broadening of the $\Delta C(V)$ curve toward negative voltages that derives from the voltage dependence of T-type channel inactivation. Thus, hypoxia-recruited T-type channels provide an additional source of Ca^{2+} entry at low voltages during stressful conditions where catecholamine secretion is potentiated (Fletcher, 2001).

Amperometric recordings induced by specifically designed KCl solutions that activate T-type channels also support the existence of an extra source of catecholamine secretion after CH. Mild depolarizations to −50 mV in 2–4 mM KCl clearly cause an increased frequency of low-voltage amperometric spikes without affecting their rising/falling phase and the total quantity of released charges. This indicates that CH and Ca^{2+} channel remodelling do not produce substantial changes to the catecholamine content of vesicles and neither affects the kinetics of catecholamine release. An increased frequency of low-voltage amperometric spikes in hypoxic cells, selectively attenuated by 50 μM Ni^{2+}, suggests that newly recruited T-type channels are effectively colocalized with the release sites and have full control of secretion at low voltages. This view is confirmed by observing that frequency, quantal size and kinetics of low-voltage amperometric spikes in RCCs are comparable to those induced by HVA channels activated by high KCl solutions (Xu & Tse, 1999; Tang *et al.* 2005). Thus, amperometry supports the view that T-type channels are coupled to exocytosis like the HVA channels and control basal exocytosis in hypoxic RCCs.

An increased basal control of exocytosis could be also due to the expression of transient receptor potential channels such as TRPC6 or any other TRP channel which could be up-regulated by hypoxia, as reported in PC12 (Tesfai *et al.* 2001) and smooth muscle cells (Lin *et al.* 2004; Wang *et al.* 2006). This possibility, however, would not account for the present findings since catecholamine release was always observed during KCl-induced depolarizations, which should not induce significant TRP channel openings. In addition, we never observed increased basal levels of amperometric spikes in the absence of stimuli (Fig. 9), while a hypothetical up-regulation of TRP channels would predict increased intracellular [Ca^{2+}] and enhanced secretory basal activity (Obukhov & Nowycky, 2002). Finally, chromaffin cells do not express TRP channels (Philipp *et al.* 2000) and there are no indications of up-regulatory effects of hypoxia on TRP channels in these cells.

A HIF-dependent pathway mediates T-type channel recruitment

Our data show clearly that as for PC12 cells (Del Toro *et al.* 2003) the mechanism of T-type channel recruitment by CH involves the activation of HIFs. Indeed, the iron chelating agent DFX, which stabilizes HIFs by inhibiting prolyl-hydroxylases and preventing its proteasomal degradation (Semenza, 2004; Cummins & Taylor, 2005), perfectly mimics the action of CH. We found no significant differences in using DFX or CH to induce T-type channels and associated exocytosis. In both cases, overnight incubation was sufficient to recruit T-type channel densities comparable to those induced by long-term treatments with cAMP, which required longer times (> 3 days) and the involvement of Epac cAMP-receptor proteins (Novara *et al.* 2004). This suggests that the two mechanisms, HIF-induced and cAMP-Epac-mediated recruitment of T-type channels, may proceed through two different pathways involving transcriptional and post-transcriptional mechanisms. Of relevance is the fact that, as suggested by Del Toro *et al.* (2003), the 5′-flanking region of the α_{1H} gene possesses a number of sequences compatible with hypoxia-responsive elements that may represent the promoter region for α_{1H} gene transcription. A second relevant issue is the non-involvement of PKA in both processes, suggesting that T-type channel remodelling is mainly PKA independent regardless of the triggering stimuli. This is in line with the observation that CH down-regulates PKA enzyme activity in PC12 cells (Beitner-Johnson *et al.* 1998; Kobayashi *et al.* 1998) and cardiomyocytes (Fung *et al.* 2002), preventing L-type channel potentiation via β-adrenergic stimulation.

The reported recruitment of T-type channels in RCCs supports the idea that CH causes an increased excitability of adrenal medulla cells and sustained catecholamine release that is part of the body's sympathetic response to CH and is responsible for key cardiovascular changes (Johnson *et al.* 1983; Bao *et al.* 1997; Fletcher, 2001) and stressful pathological conditions in neuronal (Chung *et al.* 1993; Tsakiridou *et al.* 1995) and neuroendocrine tissues (Mariot *et al.* 2002; Del Toro *et al.* 2003). Recruitment of T-type channels appears to be a genuine marker of stressful conditions in which the low threshold of activation and slow deactivation contribute to regulate cell excitability, autorhythmicity and vesicular neurotransmitter release (Pérez-Reyes, 2003; Carbone *et al.* 2006).

References

Bao G, Metreveli N, Li R, Taylor A & Fletcher E (1997). Blood pressure response to chronic episodic hypoxia: role of the sympathetic nervous system. *J Appl Physiol* **83**, 95–101.

Beitner-Johnson D, Leibold J & Millhorn DE (1998). Hypoxia regulates the cAMP- and Ca^{2+}/calmodulin signaling systems in PC12 cells. *Biochem Biophys Res Commun* **241**, 61–66.

Bijlenga P, Liu J-H, Espinos E, Haenggeli C-A, Fischer-Lougheed J, Bader CR & Bernheim L (2000). T-type α1H Ca^{2+} channels are involved in Ca^{2+} signaling during terminal differentiation (fusion) of human myoblasts. *Proc Natl Acad Sci U S A* **97**, 7627–7632.

Bournaud R, Hidalgo J, Yu H, Jaimovich E & Shimahara T (2001). Low threshold T-type calcium current in rat embryonic chromaffin cells. *J Physiol* **537**, 35–44.

Carabelli V, Giancippoli A, Baldelli P, Carbone E & Artalejo AR (2003). Distinct potentiation of L-type currents and secretion by cAMP in rat chromaffin cells. *Biophys J* **85**, 1326–1337.

Carbone E & Lux D (1987). Single low-voltage-activated calcium channels in chick and rat sensory neurones. *J Physiol* **386**, 571–801.

Carbone E, Marcantoni A, Giancippoli A, Guido D & Carabelli V (2006). T-type channels-secretion coupling: evidence for a fast low-threshold exocytosis. *Pflugers Arch* **453**, 373–383.

Cesetti T, Hernandez-Gujio JM, Baldelli P, Carabelli V & Carbone E (2003). Opposite action of β_1- and β_2-adrenergic receptors on Ca_V1, L-channel current in rat adrenal chromaffin cells. *J Neurosci* **23**, 73–83.

Chouabe C, Espinosa L, Megas P, Chakir A, Ropugier O, Freminet A & Bonvallet R (1997). Reduction of $I_{Ca,L}$ and I_{to1} density in hypertrophied right ventricular cells by simulated high altitude in adult rats. *J Mol Cell Cardiol* **29**, 193–206.

Chung J-M, Huguenard JR & Prince DA (1993). Transient enhancement of low-threshold calcium current in thalamic relay after corticectomy. *J Neurophysiol* **702**, 20–27.

Crunelli V, Tóth TI, Cope DW, Blethyn K & Hughes SW (2005). The 'window' T-type calcium current in brain dynamics of different behavioral states. *J Physiol* **562**, 121–129.

Cummins EP & Taylor CT (2005). Hypoxia-responsive transcription factors. *Pflugers Arch* **450**, 363–371.

Del Toro R, Levitsky KL, López-Barneo J & Chiara MD (2003). Induction of T-type calcium channel gene expression by chronic hypoxia. *J Biol Chem* **278**, 22316–22324.

Fearon IM, Randall AD, Pérez-Reyes E & Peers C (2000). Modulation of recombinant T-type Ca^{2+} channels by hypoxia and glutathione. *Pflugers Arch* **441**, 181–188.

Fletcher EC (2001). Physiological consequences of intermittent hypoxia: systemic blood pressure. *J Appl Physiol* **90**, 1600–1605.

Fung M-L, Li H-Y & Wong T-M (2002). Forskolin fails to activate L-type calcium current in hypertrophied cardiomyocytes of chronically hypoxic rats. *Life Sci* **70**, 1801–1809.

Giancippoli A, Novara M, de Luca A, Baldelli P, Marcantoni A, Carbone E & Carabelli V (2006). Low-threshold exocytosis induced by cAMP-recruited $Ca_v3.2$ (α_{1H}) channels in rat chromaffin cells. *Biophys J* **90**, 1830–1841.

Green KN, Boyle JP & Peers CJ (2002). Hypoxia potentiates exocytosis and Ca^{2+} channels in PC12 cells via increased amyloid β-peptide formation and reactive oxygen species generation. *J Physiol* **541**, 1013–1023.

Hempleman SC (1996). Releasable pools and the kinetics of exocytosis in adrenal chromaffin cells. *J Neurophysiol* **76**, 1880–1886.

Hollins B & Ikeda SR (1996). Inward currents underlying action potentials in rat adrenal chromaffin cells. *J Neurophysiol* **76**, 1195–1211.

Horrigan FT & Bookman RJ (1994). Releasable pools and the kinetics of exocytosis in adrenal chromaffin cells. *Neuron* **13**, 1119–1129.

Jan Y & Jan YN (1976). L-Glutamate as an excitatory transmitter at the drosophila larval neuromuscular junction. *J Physiol* **262**, 215–236.

Johnson TS, Young JB & Landsberg L (1983). Sympathoadrenal responses to acute and chronic hypoxia in the rat. *J Clin Invest* **71**, 1263–1272.

Kobayashi S, Beitner-Johnson D, Laura Conforti L & Millhorn DE (1998). Chronic hypoxia reduces adenosine A_{2A} receptor-mediated inhibition of calcium current in rat PC12 cells via downregulation of protein kinase. *J Physiol* **512**, 351–363.

Lee JH, Gomora JC, Cribbs LL & Perez-Reyes E (1999). Nickel block of three cloned T-type calcium chanels: low concentrations selectively block alpha 1H. *Biophys J* **77**, 3034–3042.

Lewis CA (1979). Ion concentration-dependence of the reversal potential and the single channel conductance of ion channels at the frog neuromuscular junction. *J Physiol* **286**, 417–445.

Lin M-J, Leung GPH, Zhang W-M, Yang X-R, Yip K-P, Tse C-M & Sham JSK (2004). Chronic hypoxia-induced upregulation of store-operated and receptor-operated Ca^{2+} channels in pulmonary arterial smooth muscle cells. A novel mechanism of hypoxic pulmonary hypertension. *Circ Res* **95**, 496–505.

López-Barneo J, Del Toro R, Levitsky KL, Chiara MD & Ortega-Sáenz P (2003). Regulation of oxygen sensing by ion channels. *J Appl Physiol* **96**, 1187–1195.

Machado JD, Morales A, Gómez JF & Borges R (2001). cAMP modulates exocytosis kinetics and increases quantal size in chromaffin cells. *Mol Pharmacol* **60**, 514–520.

Mariot P, Vanoverbergher K, Lalevée N, Rossier MF & Prevarskaya N (2002). Overexpression of an α_{1H} ($Ca_V3.2$) T-type calcium channel during neuroendocrine differentiation of human prostate cancer cells. *J Biol Chem* **277**, 10824–10833.

McRory JE, Santi CM, Hamming KS, Mezeyova J, Sutton KG, Baillie DL, Stea A & Snutch TP (2001). Molecular and functional characterization of a family of rat brain T-type calcium channels. *J Biol Chem* **276**, 3999–4011.

Montoro RJ, Urena J, Fernández-Chacón R, Alvarez de Toledo G & López-Barneo J (1996). Oxygen sensing by ion channels and chemotransduction in single glomus cells. *J Gen Physiol* **107**, 133–143.

Neely A & Lingle C (1992). Two components of calcium-activated potassium current in rat adrenal chromaffin cells. *J Physiol* **453**, 97–134.

Novara M, Baldelli P, Cavallari D, Carabelli V, Giancippoli A & Carbone E (2004). Exposure to cAMP and β-adrenergic stimulation recruits Ca_V3 T-type channels in rat chromaffin cells through Epac cAMP-receptor proteins. *J Physiol* **558**, 433–449.

Nuss HB & Houser SR (1993). T-type Ca^{2+} current is expressed in hypertrophied adult feline left ventricular myocytes. *Circ Res* **73**, 777–782.

Obukhov AG & Nowycky MC (2002). TRPC4 can be activated by G-protein-coupled receptors and provides sufficient Ca^{2+} to trigger exocytosis in neuroendocrine cells. *J Biol Chem* **277**, 16172–16178.

Park YB, Herrington J, Babcock DF & Hille B (1996). Ca^{2+} clearance mechanisms in isolated rat adrenal chromaffin cells. *J Physiol* **492**, 329–346.

Peña F & Ramirez J-M (2005). Hypoxia-induced changes in neuronal network properties. *Mol Neurobiol* **32**, 251–283.

Pérez-Reyes E (2003). Molecular physiology of low-voltage-activated T-type calcium channels. *Physiol Rev* **83**, 117–161.

Philipp S, Trost C, Warnat J, Rautmann J, Himmerkus N, Schroth G, Kretz O, Nastainczyk W, Cavalie A, Hothi M & Flockerzi V (2000). TRP4 (CCE1) protein is part of native calcium release-activated Ca^{2+}-like channels in adrenal cells. *J Biol Chem* **275**, 23965–23972.

Schmitt R, Clozel J-P, Iberg N & Bühler FR (1995). Mibefradil reverts neointima formation after vascular injury in rats: possible role of the blockade of the T-type voltage-operated calcium channel arteriosclerosis. *Thromb Vasc Biol* **15**, 1161–1165.

Schrier AD, Wang H, Talley EM, Perez-Reyes E & Barrett PQ (2001). α_{1H} T-type Ca^{2+} channel is the predominant subtype expressed in bovine and rat zona glomerulosa. *Am J Physiol Cell Physiol* **280**, C265–C272.

Scragg JS, Fearon IM, Boyle JP, Ball SG, Varadi G & Peers C (2005). Alzheimer's amyloid peptides mediate hypoxic up-regulation of L-type Ca^{2+} channels. *FASEB J* **19**, 150–152.

Segura F, Brioso MA, Gómez JF, Machado JD & Borges R (2000). Automatic analysis for amperometrical recordings of exocytosis. *J Neurosci Methods* **103**, 151–156.

Semenza GL (2004). Hydroxylation of HIF-1-oxygen sensing at the molecular level. *Physiology* **19**, 176–182.

Sen L & Smith TW (1994). T-type Ca^{2+} channels are abnormal in genetically determined cardiomyopathic hamster hearts. *Circ Res* **75**, 149–155.

Seta KA, Yuan Y, Spicer Z, Lu G, Bedard J, Ferguson TK, Pathrose P, Cole-Strauss A, Kaufhold A & Millhorn DE (2004). The role of calcium in hypoxia-induced signal transduction and gene expression. *Cell Calcium* **36**, 331–340.

Sjodin RA (1980). Contribution of Na/Ca transport to the resting membrane potential. *J Gen Physiol* **76**, 99–108.

Smirnov SV, Robertson TP, Ward JP & Aaronson PI (1994). Chronic hypoxia is associated with reduced delayed rectifier K^+ current in rat pulmonary artery muscle cells. *Am J Physiol Heart Circ Physiol* **266**, H365–H370.

Stea A, Jackson A, Macintyre L & Nurse CA (1995). Long-term modulation of inward currents in O_2 chemoreceptors by chronic hypoxia and cyclic AMP in vitro. *J Neurosci* **15**, 2192–2202.

Sun M-K & Reis DJ (1994). Hypoxia-activated Ca^{2+} currents in pacemaker neurons of rat rostral ventrolateral medulla *in vitro*. *J Physiol* **476**, 101–116.

Tabares L, Alés E, Lindau M & Alvarez de Toledo G (2001). Exocytosis of catecholamine (CA)-containing and CA-free granules in chromaffin cells. *J Biol Chem* **276**, 39974–39979.

Tang KS, Tse A & Tse FW (2005). Differential regulation of multiple populations of granules in rat adrenal chromaffin cells by culture duration and cyclic AMP. *J Neurochem* **92**, 1126–1139.

Taylor SC, Batten TFC & Peers C (1999). Hypoxic enhancement of quantal catecholamines secretion. *J Biol Chem* **274**, 31217–31222.

Tesfai Y, Brereton HM & Barritt GJ (2001). A diacylglycerol-activated Ca^{2+} channel in PC12 cells (an adrenal chromaffin cell line) correlates with expression of the TRP-6 (transient receptor potential) protein. *Biochem J* **358**, 717–726.

Tsakiridou E, Bertollini L, de Curtis M, Avanzini G & Pape H-C (1995). Selective increase in T-type calcium conductance of reticular thalamic neurons in a rat model of absence epilepsy. *J Neurosci* **152**, 3110–3117.

Wang J, Juhaszova M, Rubin LJ & Yuan XJ (1997). Hypoxia inhibits gene expression of voltage-gated K^+ channel α subunits in pulmonary artery smooth muscle cells. *J Clin Invest* **100**, 2347–2353.

Wang J, Weigand L, Lu W, Sylvester JT, Semenza GL & Shimoda LA (2006). Hypoxia inducible factor 1 mediates hypoxia-induced TRPC expression and elevated intracellular Ca^{2+} in pulmonary arterial smooth muscle cells. *Circ Res* **98**, 1528–1537.

Wyatt CN, Wright C, Bee D & Peers C (1995). O_2-sensitive K^+ currents in carotid body chemoreceptor cells from normoxic and chronically hypoxic rats and their roles in hypoxic chemotransduction. *Proc Natl Acad Sci U S A* **92**, 295–299.

Xu J & Tse FW (1999). Brefeldin A increases the quantal size and alters the kinetics of catecholamine release from rat adrenal chromaffin cells. *J Biol Chem* **274**, 19095–19102.

Acknowledgements

We thank Dr C. Franchino for preparing the cell cultures and Dr A. Giancippoli for helping with part of the experiments. We also thank Prof Josè Lopez-Barneo for stimulating discussions. This work was supported by the Italian MIUR (grant COFIN no. 2005054435 to E.C), the Regione Piemonte (grants No. A28-2005 to V.C and No. D14- 2005 to E.C) and the San Paolo IMI Foundation (grant to the NIS Center of Excellence).